

Construction of a Dynamic Adaptive Optics (AO) System Based on the Subspace Identification

H-Q. LIN^{1,2,3}, P. YANG^{1,2,*}, B. XU^{1,2}, K-J. YANG^{1,2,3} AND L-H. WEN^{1,2,3}

¹*Key Laboratory on Adaptive Optics, Chinese Academy of Sciences, Chengdu 610209, Sichuan Province, China*

²*Institute of Optics and Electronics, Chinese Academy of Sciences, Chengdu 610209, Sichuan Province, China*

³*University of Chinese Academy of Sciences, Beijing 100049, China*

Adaptive optics (AO) systems have been used in many applications such as ground-based astronomical telescopes for improving the resolution by counteracting the effects of atmospheric turbulence; however, the traditional AO system model is not good at dealing with noise interference in the closed-loop correction. This paper proposes a subspace system identification method based on errors-in-variables (EIV) to build an accurate dynamic model of AO system from measurement data with closed-loop system identification. Experimental simulation results show that the root mean squares (RMS) of the residual wavefront is obviously smaller than that of the traditional method, whether background light noise and camera readout noise exist or not. We can conclude that the identified model has good accuracy and noise disturbance compensation ability to deal with dynamic wavefront correction compared with traditional method.

Keywords: Adaptive optics (AO), dynamic model, errors-in-variables (EIV), subspace system identification

1 INTRODUCTION AND BACKGROUND THEORY

Adaptive optics (AO) systems are widely used in several scientific and medical applications, such as astronomy, laser systems and microscopes, to

*Corresponding author: E-mail: pingyang2516@163.com

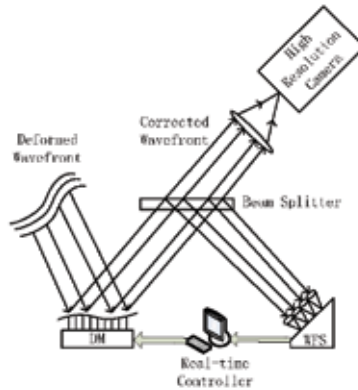


FIGURE 1
Schematic diagram showing the AO system.

improve the resolution of the image by actively sensing and compensating the optical aberration [1-2]. An AO system aims at reducing the wavefront distortions by controlling a deformable mirror (DM) that compensates for the effects of the atmospheric turbulence.

The working principle of AO system is shown in Figure. 1. The deformed wavefront arrives at the wavefront sensor (WFS), which measures the phase distortions. Then, the real-time controller computes the input signal applied to the DM for wavefront compensation. An accuracy AO system model plays an important role in closed-loop correction. At present, the model of AO system can be divided into two kinds. The first is the simplified model which usually considers the AO system as a pure delay link [3-5]. The second is the traditional model based on the influence matrix of the DM of which the parameters is tuned to make a trade-off among disturbance rejection, noise amplification, and closed-loop stability [6-7]. The simplified model does not represent the influences of the linear system link, and the parameters of traditional model are more complex in closed-loop correction. Both the simplified model and the traditional method based on the influence matrix of the DM are difficult to be implemented by the modern control algorithm which need the accurate model base.

In order to solve the above problems, the technology of subspace system identification is widely used in AO systems to build accurate dynamical models [8]. Looze [9] and Looze *et al.* [10] were the first to build a dynamic mathematical model of the AO system by use of the mathematical method and evaluate the performance of the closed-loop system by simulations [9-10]. Chiuso *et al.* [11, 12] and Song *et al.* [13] apply a closed-loop subspace identification approach for the AO system based on the measurement data. These methods can build accuracy AO system models. These examples all assume that input and output have no noise interference, which, however, is not the case in practice.

The problem of identifying a model from noisy input-output observations is known as the errors-in-variables (EIV) problem [14-16]. Since the AO system is a multi-input and multi-output system, and its dynamic model has delay link and linear link, the method of subspace identification is fairly suitable to obtain an accuracy dynamic model of the AO system. Because of the unique advantages, subspace identification has attracted a lot of attentions in the last two decades [17-18]. Subspace identification algorithm is generally divided into four categories: the canonical variate algorithm (CVA) [19], the numerical algorithms for subspace state space system identification (N4SID) [20], the multivariable output-error state space (MOESP) [21], and the instrumental variable-subspace state space system identification (IV-4SID) [22]. All of these methods estimate the range space of the observability matrix, and then obtain the matrix of the state-space form by either estimating the observability matrix or estimating the state sequence. Although these methods are easy to implement, these methods, in principle, are only applicable in open-loop identification and cannot build an accuracy dynamic model of the AO system.

This paper proposes the method of a MOESP-variant subspace identification based on the EIV closed-loop identification to identify an accuracy dynamic AO system model from measurement data, so as to solve the closed-loop identification problem of identifying an accuracy dynamic model of the AO system from noisy input-output observations. It will give a model foundation for the design of AO system controller.

2 ERRORS-IN-VARIABLES (EIV) SUBSPACE IDENTIFICATION

2.1 Problem statement

The AO system has been described in Figure 2. It is composed of one WFS, one DM and one controller unit. The symbols in Figure 2 have the following meanings: signal μ_k is the control input (the voltages applied to the DM); y_k is the control output (the residual wavefront phase); and w_k and v_k are the measurement noises which have been added for identification. The input and output data are corrupted by additional noise. The scenario under consideration is depicted in Figure 3, where the identified AO system is modelled by the following linear time-invariant (LTI) state space model of finite order:

$$x_{k+1} = Ax_k + B\tilde{u}_k \quad (1a)$$

and

$$\tilde{y}_k = Cx_k + D\tilde{u}_k \quad (1b)$$

where A , B , C and D is the state space realization of the AO system, and x_k is the state sequence of the AO system.

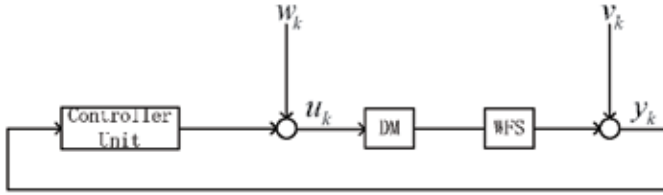


FIGURE 2
The signal block diagram of the AO system.



FIGURE 3
Block schematic diagram of the general EIV identification problem.

The observations available for identification are the measured input μ_k and the measured output y_k . They are related to \tilde{y}_k and \tilde{u}_k , as follows:

$$u_k = \tilde{u}_k + w_k \tag{2a}$$

and

$$y_k = \tilde{y}_k + v_k \tag{2b}$$

where w_k and v_k represent noise disturb of the AO system. In this paper they are white noise.

So, the EIV identification problem of the AO systems: given the corrupted input and output measurements $\{\mu_k\}$ and $\{y_k\}$ of the unknown AO system. Determine, using the ergodic-algebraic framework thus: (i) an estimate of the AO system order n ; and (ii) a consistent estimate of the quadruple of system matrices (A, B, C, D) up to a similarity transformation; this equivalent quadruple is denoted by (A_T, B_T, C_T, D_T) .

2.2 Subspace identification

The problem described in the previous section will be solved in the framework of subspace identification methods. The algorithm of this paper is based on a family of algorithms known as MOESP [23–25]. The marked character-

istic of the MOESP family of algorithms is that the state space model is estimated in two steps. The first step, the extended observability matrix Γ_s of the system is estimated. According to the matrix Γ_s , we can estimate the order of the system and compute the value of A and C . The second step, the matrices of B and D can be obtained based on estimated A and C employing the method of the linear least-squares.

For the subspace identification algorithm, the data of input and output are stored in a structured block Hankel matrix:

$$U_{j,s,N} = \begin{bmatrix} u_j & u_{j+1} & \cdots & u_{j+N-1} \\ u_{j+1} & u_{j+2} & \cdots & u_{j+N} \\ \vdots & \vdots & \ddots & \vdots \\ u_{j+s-1} & u_{j+s} & \cdots & u_{j+N+s-2} \end{bmatrix} \quad (3)$$

where the first subscript of $U_{j,s,N}$ indicates the time index of the top left-hand side element of the matrix, whereas the subscripts s and N indicate, respectively, the number of the block rows and columns. In the same way, the output sequence $\{y_k\}$ and the noise sequences $\{w_k, v_k\}$ are the same as $U_{j,s,N}$. These block Hankel matrices will, respectively, be denoted by $Y_{j,s,N}$, $W_{j,s,N}$ and $V_{j,s,N}$. According to Equations (1a), (1b), (2a) and (2b), these Hankel matrices can be shown by

$$Y_{j,s,N} = \Gamma_s X_{j,N} + H_s U_{j,s,N} - H_s W_{j,s,N} + V_{j,s,N} \quad (4)$$

where H_s is block Toeplitz matrix. These matrices are

$$\Gamma_s = \begin{bmatrix} C \\ CA \\ \vdots \\ CA^{s-1} \end{bmatrix}, X_{j,N} = [x_j \quad \cdots \quad x_{j+N-1}] \quad (5)$$

$$H_s = \begin{bmatrix} D & & & \\ CB & D & & \\ \vdots & & \ddots & \\ CA^{s-2}B & & & D \end{bmatrix}$$

As mentioned before, once an estimation of Γ_s is obtained, the matrix pair (A, C) will be estimated.

Now, according to subspace identification PI-MOESP algorithm, we can obtain

$$\begin{bmatrix} U_{s+1,s,N} \\ U_{1,s,N} \\ Y_{s+1,s,N} \end{bmatrix} = \begin{bmatrix} R_{11}^N & 0 & 0 \\ R_{21}^N & R_{22}^N & 0 \\ R_{31}^N & R_{32}^N & R_{33}^N \end{bmatrix} \begin{bmatrix} Q_1^N \\ Q_2^N \\ Q_3^N \end{bmatrix} \quad (6)$$

then, according to the theory of the subspace identification, we make use of RQ factorization to have

$$Y_{s+1,s,N} /_{U_{s+1,s,N}} U_{1,s,N} = R_{32}^N Q_2^N \quad (7)$$

The left hand side of the Equation (7) indicates that the row space of $Y_{s+1,s,N}$ along the row space of $U_{s+1,s,N}$ projects on the row of space of $U_{1,s,N}$. Then, according to singular value decomposition (SVD) factorization, we can obtain

$$R_{32}^N = U_n S_n \quad (8)$$

where U_n can also be denoted by

$$\Gamma_s = U_n = \begin{bmatrix} C_T \\ C_T A_T \\ \vdots \\ C_T A_T^{s-1} \end{bmatrix} \quad (9)$$

and so the matrix C_T equals the first l (l is the number of output) rows of U_n , that is $C_T = U_n(1:l,:)$. The matrix A_T is computed by

$$U_n(1:(s-1)l,:)A_T = U_n(l+1:sl,:) \quad (10)$$

Now, the matrix pair (A, C) has been estimated. Then, we will compute the matrix pair (B, D) . Given the matrix A_T and C_T , the output \tilde{y}_k of the state space model given in Equation (1b) can be written as

$$\tilde{y}_k = CA_T^k x_T(0) + \left(\sum_{\tau=0}^{k-1} u_\tau \otimes C_T A_T^{k-\tau-1} \right) \text{vec}(B_T) + \left(u_k \otimes I_l \right) \text{vec}(D) \quad (11)$$

let A_T and C_T denote the estimates of the A and C computed in the previous step. Now, taking

$$\phi(k)^T = \left[C_T A_T \left(\sum_{\tau=0}^{k-1} u(\tau)^T \otimes C_T A_T^{k-\tau-1} \right) \left(u(k)^T \otimes I_l \right) \right] \quad (12)$$

and

$$\theta = \begin{bmatrix} x_T(0) \\ \text{vec}(B_T) \\ \text{vec}(D) \end{bmatrix} \quad (13)$$

we can solve for θ in a least-squares setting:

$$\min \frac{1}{N} \sum_{k=0}^{N-1} \left\| y(k) - \phi(k)^T \theta \right\|_2^2 \quad (14)$$

and, therefore, B_T and D_T can be estimated.

Now, we can obtain the AO system interaction matrix (DC gain of the identified AO system model) according to (A_T, B_T, C_T, D_T) :

$$R_{id} = C_T (I - A_T)^{-1} B_T + D_T \quad (15)$$

3 ADAPTIVE OPTICS (AO) SYSTEM IDENTIFICATION

The goal of this paper is to identify an accurate AO system model using off-line closed-loop subspace identification. We address the identification of a dynamic model linking the control action from the control input $u(k)$ to the control output $y(k)$ for the AO system, in Figure. 2.

The DM has 61 actuators and the WFS has 64 sub-apertures. Each sub-aperture has two directions of slop measurements: x axis direction and y axis direction. Because the AO system is a kind of MIMO system with 61 inputs and 128 outputs (input $m=61$ and output $l=128$), we use a method of subspace approach. As far as memory requirements are concerned, this ideally allows to perform identification with an arbitrarily large number of data points; increasing the number of data is just a matter of computation time. The identification data of this paper is obtained from AO system closed correction based on traditional method in experiment. The data point N of this paper used in experiment is roughly 15000. The noise w_k and v_k can be represented with zero-mean white Gaussian noise in Figure. 3. Due to closed-loop identification, the controller in the control loop is a simple PI controller. The transfer from the DM surface input $u(k)$ to the residual wavefront phase output $y(k)$ can be considered linear and a linear dynamic model can be identified for the controller design. In general, the AO system model can be represented in discrete state space form, for example as equation (1).

According to the section 2, the AO system model is identified in three steps: (i) a observability matrix Γ_s can be estimated from the input and output Hankel matrices by RQ factorization; (ii) the estimated matrix pair (A_T, C_T) of the matrix pair (A, C) and the order of the AO system can be computed based on the matrix Γ_s ; and (iii) the estimated matrix pair (B_T, D_T) of the matrix pair (B, D) can be obtained based on the estimated matrix pair (A_T, C_T) employing the least-squares method.

The accuracy of the identified AO system model is evaluated by calculating the variance accounted for (VAF) of the model, which is defined as

$$\text{VAF} = \left(1 - \frac{\text{var}(y_{real}(k) - y_{id}(k))}{\text{var}(y_{real}(k))} \right) \times 100\% \quad (16)$$

where, $y_{real}(k)$ is the real output of the AO system model and $y_{id}(k)$ is the output of the identified AO system model. If the accuracy of the identified model is higher, the VAF should be closed to 100%. We can obtain the following Figure. 4 according to Equation (16), it shows that the accuracy of identified AO systems model is very high.

4 RESULTS AND DISCUSSION

The WFS is S-H WFS based on the geometric diffraction and the DM is based on influence function in this paper. If input signal V_j is the control voltage added to the j th actuator of the DM, the average gradient in the sub-apertures of the WFS is

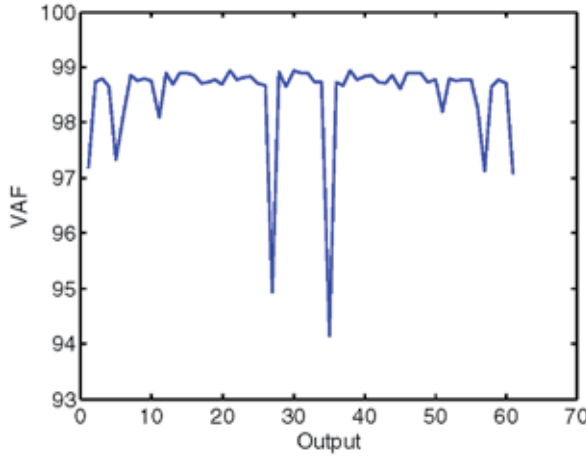


FIGURE 4
The VAF of the identified AO system model.

$$\left\{ \begin{aligned} G_x(i) &= \sum_{j=1}^t V_j \frac{\iint_{S_i} \frac{\partial R_j(x,y)}{\partial x} dx dy}{S_i} = \sum_{j=1}^t V_j R_{xj}(i) \\ G_y(i) &= \sum_{j=1}^t V_j \frac{\iint_{S_i} \frac{\partial R_j(x,y)}{\partial y} dx dy}{S_i} = \sum_{j=1}^t V_j R_{yj}(i) \end{aligned} \right. , i = 1, 2, 3, \dots, m \quad (17)$$

where $R_i(x,y)$ is the j th actuator influence function of the DM; t is the number of the actuators; m is the number of the sub-apertures of the WFS; and S_i is the i th sub-aperture normalization area. According to the linear relationship between sub-apertures gradient G of the WFS and actuators voltage V of the DM, the equation (17) can be written as

$$G = R * V \quad (18)$$

where R is the influence matrix from the WFS to the DM, which can be calculated based on the Fourier transformation theoretically or based on the WFS experimentally. According to Equation (18), we can then obtain

$$V = R^\dagger * G \quad (19)$$

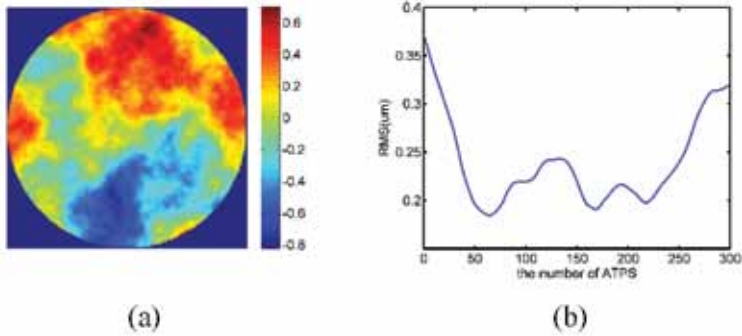


FIGURE 5

(a) The two-dimensional (2-D) image of the incident ATPS and (b) the RMS of the incident ATPS.

where V the control voltage of the DM which is corresponding to the current wavefront; and R^\dagger is the transfer matrix which is the pseudo inverse of matrix R . This is the so called traditional method.

Then, we validate the identified AO system model in the closed-loop correction through a series of simulations. In the closed-loop correction, we first use the identified model and traditional model to calculate the control voltage signal V according to Equation (15) and Equation (19), which is corresponding to the current residual wavefront, respectively. Next, we make use of the following same PI controller ($pi_a=0.998$, $pi_b=0.8$) to obtain the final control voltage signal V_{end} applied to the DM, respectively:

$$V_{end} = pi_a * V(k-1) + pi_b * V \quad (20)$$

In order to compare the accuracy and reliability of identified model, a set of dynamic atmospheric turbulence phase screen (ATPS) (which is exactly different from the identification data.) is used as external interference input wavefront according to Kolmogorov atmospheric turbulence when the wind speed is 5 m/s, seeing Figure. 5. The parameters of atmospheric turbulence is $D/r_0=7$, and the sampling rate of the WFS camera is 1000 Hz. Next, we respectively use identified model and traditional model to correct the same set of ATPS whether with the background light noise and camera readout noise or without noise.

In the absence of noise interference, the correction results of different model and the residual wavefront after correction are shown in Figure. 6, and the root mean squares (RMS) of the two models are all most the same in Figure. 7. We can conclude that the identified model has high accuracy

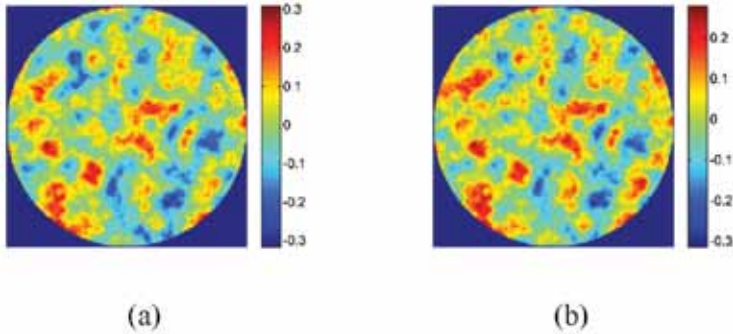


FIGURE 6

Residual wavefront images when (a) corrected by the traditional model, $\text{RMS}=0.10\ \mu\text{m}$ and (b) corrected by the identified model, $\text{RMS}=0.08\ \mu\text{m}$.

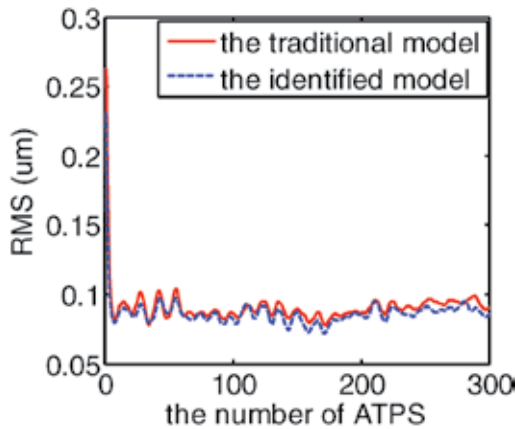


FIGURE 7

The RMS value of the residual wavefront after being corrected by the DM.

and good correction ability for dynamic ATPS from Figure 6. From Figure 7, the RMS of the residual wavefront based on identified model is $0.08\ \mu\text{m}$, while that of traditional model is $0.1\ \mu\text{m}$. The correction result of the identified model is a little better than that of the traditional model.

When the S-H WFS detects the wavefront, the camera generates the background light noise and camera readout noise [26]; therefore, in the actual AO system, in addition to the influence of external interference, there is also internal noise interference such as the background light noise and camera readout noise. In order to verify the compensation ability of the identified model, we take the background light noise and camera readout

noise as examples to analyse and compare the performance of the identified AO system model in which the background light noise obey the Poisson distribution with a mean value of 1 and the camera readout noise is zero-mean Gaussian distribution with a variance of 0.1. Next, we have to verify our identified AO model in the presence of both. The incident ATPS is shown in Figure. 5.

The different model correction results and the far field after correction in presence of both noises are shown in Figure. 8. The RMS of two kinds of model in presence of both noises are described in Figure. 9. We can conclude that the RMS and correction effect of the identified model are obviously better than that of that of the traditional method from Figure 8 and Figure 9. It can be explained that the identified model not only has good correction effect but also has a strong ability to suppress noise interference in the presence of background light noise and camera readout noise from Figure 8 and Figure 9.

Figure. 9 shows that the correction effect of the identified AO system model is much better than that of the traditional model under noise conditions. As can be seen from Figure. 9, although the RMS value of the identified model is a bit large in several places, it is generally better than that of the traditional model in presence of the background light noise and camera readout noise. Comparing with free noise in Figure. 7, although the RMS value of the identified model is improved a little, it is still less than 0.1 μm , while that of the traditional model is obviously poor. In a word, the RMS of the identified AO system model is much better than that of the traditional method, whether with the background light noise and camera readout noise or without noise in Table. 1.

5 CONCLUSIONS

We propose a method of closed-loop subspace system identification based on errors-in-variables (EIV) model to build an accurate dynamic model of adaptive optics (AO) system. Through a series of simulations, we obtain that the identified AO system model is very accurate and has a strong compensation ability and robustness. The root mean square (RMS) of residual wavefront after correction is obviously smaller than that of the traditional method.

Further work will include exploring the possibility of using such models for the purpose of controller design.

6 ACKNOWLEDGMENTS

This work has been supported by the Key Scientific Equipment Development Project of China (No. ZDYZ2013-2), the Outstanding Young Scientists, Chi-

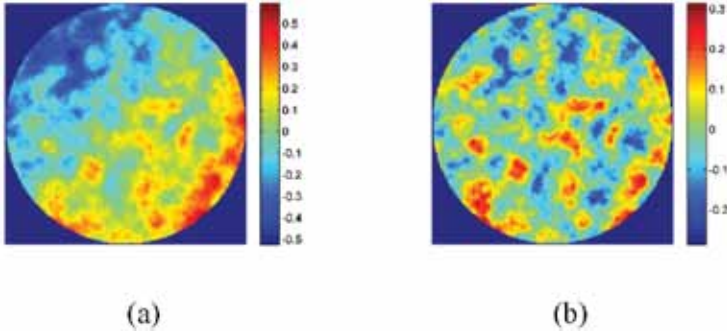


FIGURE 8 Images of the residual wavefront (a) after being corrected by the traditional model, $RMS=0.20\ \mu m$ and (b) after being corrected by the identified model, $RMS=0.09\ \mu m$.

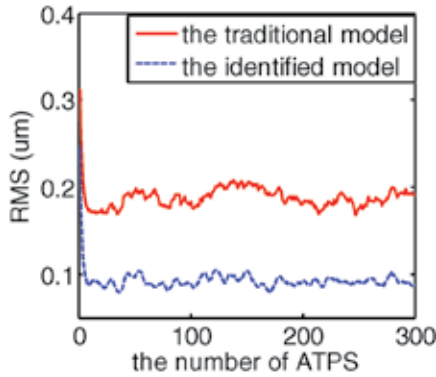


FIGURE 9 The RMS value of the residual wavefront after being corrected through 300 iterations in the presence of camera readout noise and background light noise.

TABLE 1 Noise values.

RMS (Initial ATPS is $0.36\ \mu m$)	Free of Noise (μm)	Background Light Noise and Camera Readout Noise (μm)
The traditional model	0.10	0.20
The identified model	0.08	0.09

nese Academy of Sciences and Youth Innovation Promotion Association, the National Defense Innovation Found of Chinese Academy of Sciences (CXJJ-16M208).

REFERENCES

- [1] Hardy J.W. *Adaptive Optics for Astronomical Telescopes*. Oxford: Oxford University Press. 1998.
- [2] Roddier F. *Adaptive Optics in Astronomy*. Cambridge: Cambridge University Press. 1999.
- [3] Dessenne C., Madec P.Y. and Rousset G. Optimization of a predictive controller for closed-loop adaptive optics. *Applied Optics* **37**(21) (1998), 4623-4633.
- [4] Dessenne C., Madec P.Y. and Rousset G. Modal prediction for closed-loop adaptive optics. *Optics Letters* **22**(20) (1997), 1535-1537.
- [5] Looze D.P. Structure of LQG controllers based on a hybrid adaptive optics system model. *European Journal of Control* **17**(3) (2011), 237-248.
- [6] Ellerbroek B.L., Van Loan C., Pitsianis N.P. and Plemmons R.J. Optimizing closed-loop adaptive-optics performance with use of multiple control bandwidths. *Journal of the Optical Society of America A: Optics, Image Science and Vision* **11**(11) (1994), 2871-2886.
- [7] Gendron E. and Léna P. Astronomical adaptive optics. I Modal control optimization. *Astronomy and Astrophysics* **291**(1) (1994), 337-352.
- [8] Hinnen K. and Verhaegen M. Exploiting the spatiotemporal correlation in adaptive optics using data-driven H2-optimal control. *Journal of the Optical Society of America A: Optics, Image Science and Vision* **24**(6) (2007), 1717-1725.
- [9] Looze D.P. Linear-quadratic-Gaussian control for adaptive optics systems using a hybrid model. *Journal of the Optical Society of America A: Optics, Image Science and Vision* **26**(1) (2009), 1-9.
- [10] Looze D.P., Kasper M., Hippler S. and Beker O. Optimal compensation and implementation for adaptive optics systems. *Experimental Astronomy* **15**(2) (2003), 67-88.
- [11] Chiuso A., Muradore R. and Marchetti E. Dynamic calibration of adaptive optics systems: A system identification approach. 47th *IEEE Conference on Decision and Control*. 9-11 December 2008, Cancun, Mexico. TuB04.5
- [12] Chiuso A., Muradore, R. and Fedrigo E. Adaptive optics systems: A challenge for closed loop subspace identification. 2007 *American Control Conference* 9-13 July 2007, New York, NY., USA. pp. 111-115.
- [13] Song H., Fraanje, R., Schitter G., Vdovin G. and Verhaegen M. Controller design for a high-sampling-rate closed-loop adaptive optics system with piezo-driven deformable mirror. *European Journal of Control* **17**(3) (2011), 290-301.
- [14] Verhaegen M. and Dewilde, P. Subspace model identification Part I: The output-error state space model identification class of algorithms. *International Journal of Control* **56**(5) (1992), 1187-1210.
- [15] Moonen M. and Vandewalle J. A QSVD approach to on- and off- line state space identification. *International Journal of Control* **51**(5) (1990), 1133-1146.
- [16] Huffel V. and Vandewalle J. Comparison of total least squares and instrumental variable methods for parameter estimation of transfer function models. *International Journal of Control* **50**(4) (1989), 1039-1056.
- [17] Gustafsson T. Subspace identification using instrumental variable techniques. *Automatica* **37**(12) (2001), 2005-2010.
- [18] Chiuso A. The role of vector autoregressive modeling in predictor-based subspace identification. *Automatica* **43**(6) (2007), 1034-1048.
- [19] van Overschee P. and De Moor B. *Subspace Identification for Linear Systems: Theory, Implementation, Applications*. Boston: Kluwer Academic. 1996.
- [20] Verhaegen M. and Verdult V. *Filtering and System Identification: A Least Squares Approach*. Cambridge: Cambridge University Press. 2007.
- [21] Chiuso A. On the relation between CCA and predictor -based subspace identification. *IEEE Transactions on Automatic Control* **52**(10) (2007), 1795-1812.
- [22] Viberg M. Subspace-based methods for the identification of linear time-invariant systems. *Automatica* **31**(12) (1995), 1835-1851.

- [23] Chou C.T. and Verhaegen M. Subspace algorithms for the identification of multivariable dynamic error-in-variables models. *Automatica* **33**(10) (1997), 1857-1869.
- [24] Chou C.T. and Verhaegen M. Subspace-based methods for the identification of multivariable dynamic errors-in-variables models. *Proceedings of the 35th IEEE Conference on Decision and Control*. 13 December 1996, Kobe, Japan. pp. 3636-3641.
- [25] Verhaegen M. and Westwick D. Identifying MIMO Hammerstein systems in the context of space model identification methods. *International Journal of Control* **63**(2) (1996), 331-349.
- [26] Ma X.Y., Rao C.H. and Zheng H.Q. Error analysis of CCD-based point source centroid computation under the background light. *Optics Express* **17**(10) (2009), 8525-8541.